

Textile reinforced concrete – overview, experimental and theoretical investigations

U. Häussler-Combe & F. Jesse & M. Curbach

Department of Civil Engineering, Dresden University of Technology, Germany

ABSTRACT: Textile reinforced concrete offers a new innovative technology to strengthen or repair concrete structures with thin layered composites of fine grained concrete and fabrics of high strength glass fibres or multifilament rovings respectively. Regarding the structural behavior, different mechanisms of bond play an essential role. These bond mechanisms are discussed with some details, considering experimental investigation, mechanical and numerical models and some numerical calculations.

Keywords: textile reinforced concrete, strengthening, bond, roving, filament

1 INTRODUCTION

Regarding strengthening or repair of existing concrete structures it may be highly desirable to have very thin additional load carrying layers applied to structures. This cannot be realized with steel reinforcement, as steel rebars require an additional layer width of at least roughly 5 cm. As an alternative a textile reinforcement consisting of fabrics of alkali-resistant glass fibres may be considered. Such fabrics are thin compared to steel bars and do not suffer from corrosion when exposed to common atmospheric conditions. An additional concrete cover is not necessary as a corrosion protection.

Assembly of textile concrete layers to existing concrete structures may be done with air placed concrete or shotcrete respectively. A first layer is applied by well known techniques. Then a fabric is immediately pressed against this wet concrete layer with simple tools, e.g. a roller. The fabric should be fixed – even on bottom side of slabs – due to its adhesion with the wet mortar material. A further concrete layer is applied and a further fabric is possible. This may be repeated several times and results in a laminated concrete structure. With this short description a new innovative technology to strengthen or repair concrete structures is outlined. An application example is described by Curbach & Brückner (2003).

The general technology concept has a number of detail problems. Regarding mechanical behavior this main regards bond between cement matrix and textile reinforcement, which will be a major item of the following. In section two some aspects of textile reinforcement structural behavior will be described with a special focus on bond. Some experimental results for textile concrete tension plates will be shown in section three. These results are compared with numerical calculations in section four. A conclusion is given in section five.

2 STRUCTURAL BEHAVIOR ASPECTS

2.1 *Materials*

Glass fibres or rovings respectively consist of up to 2000 glass filaments of a diameter of roughly 10 .. 25 μm . The glass material is alkali resistant to sustain long term embedding into a cementitious matrix. Uniaxial tensile strength of a single filament amounts roughly to 2000 N/mm^2 with $E_f \approx 80000 \text{ N}/\text{mm}^2$. This is reduced by at least 25% up to 50% for a multi filament fibre, which is presumably caused by particular bond effects.

A mortar like fine grained concrete with a maximum aggregate size of about 1 mm is used as a matrix. Type III Cement, fly ash and some pozzolans are used as binding material. Of course also water and superplastizer belong to the mixture. The compressive strength and bending strength values

are app. 80 N/mm and 7 N/mm² respectively with $E_c \approx 30000$ N/mm². So this is a very common mixture for glass fibre reinforced concrete. In terms of a meso-level approach the following components have to be considered for the composite material:

- Matrix of fine grained concrete.
- Single filaments bundled in a roving.
- Transition zone between existing concrete structure and new layer of textile concrete.
- Transition zones between fine grained concrete and filaments.
- Transition zones between filaments.

The different transition zones or bond in a widespread variation respectively has a crucial part for the behavior of textile concrete.

2.2 Outline of bond behavior

Corresponding to the transition zones at least three bond types have to be considered:

1. Bond between old existing concrete and new fine grained concrete matrix.
2. Bond between concrete matrix and filaments.
3. Bond between filaments.

Bond between new and old concrete may be characterized by adhesion tensile strength and shear strength. These properties are strongly influenced by the pretreatment of the existing concrete surface. Experimental and theoretical investigations were performed by Ortlepp & Curbach (2003). This type of bond will not be discussed in the following, as there are a lot of similarities compared to other techniques with strengthening layers and the mechanisms are quite different compared to the other two types.

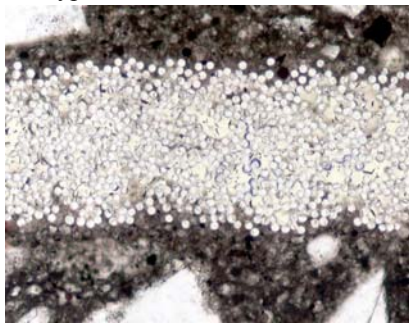


Figure 1. Cross section of a roving in concrete.

Regarding the bond types 2 and 3 it has to be considered, that rovings may not retain their original geometric shape upon embedding into mortar, as their constituent filaments are only weakly con-

nected to each other by the sizing. There is no sharp boundary between roving and confining concrete but a zone where concrete mixes with the outer filaments of a roving, see Figure 1. In contrast central filaments of a roving are not affected by fine concrete, so that bond between filaments has the major contribution.

Principally there are two bond mechanisms, adhesion and friction. Support of concrete by ribs as with steel reinforcement does not take place. Bond between filaments is dominated by friction (Littwin 2001), while both adhesion and friction contribute to bond between concrete matrix and filaments. Bond of type 2 or 3 is advisably described in a format

$$\tau = C_R \cdot f(s) \quad (1)$$

where τ = bond stress; C_R = circumference of reinforcement, s = slip between reinforcement element and concrete matrix. A reinforcement element may be a single filament, a group of filaments or a roving. Experimental investigations about the behavior of these bond types were performed by Bartos (1980), Banholzer (2001), Reinhardt & Krüger (2001). The results may be adequately approximated by a multilinear form as shown in Figure 2, with a peak value, a softening part and a final value.

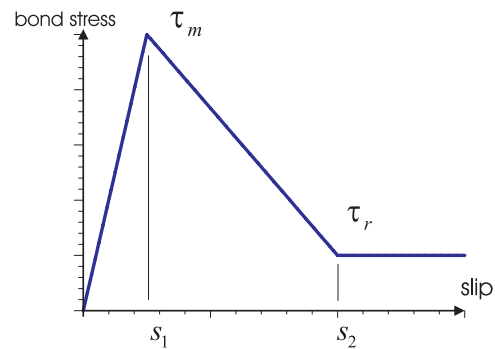


Figure 2. Typical bond behavior.

This is described in a form

$$\tau = \begin{cases} \tau_m \cdot s / s_1 & s < s_1 \\ \frac{\tau_m - \tau_r}{s_2 - s_1} \cdot s + \frac{\tau_m s_2 - \tau_r s_1}{s_2 - s_1} & s_1 \leq s \leq s_2 \\ \tau_r & s_2 < s \end{cases} \quad (2)$$

where s_1 = slip with the maximum bond, τ_m = maximum bond stress value, s_2 = slip where residual value of bond stress is reached, τ_r = residual bond stress value. Appropriate values are given by $\tau_m = 10 \text{ MN/m}^2$, $s_1 = 5 \text{ }\mu\text{m}$, $\tau_r = 3 \text{ MN/m}^2$, $s_2 = 100s_1$ for bond between concrete matrix and filaments and $\tau_m = \tau_r = 3 \text{ MN/m}^2$, $s_1 = s_2 = 5 \text{ }\mu\text{m}$ for bond between filaments.

2.3 Meso-models of bond behavior

Foregoing experimentally based observations imply an integral approach from a macroscopic point of view. Further observations from a mesoscopic or even microscopic point of view (Butler 2003, Brameshuber & Banholzer 2003, Mäder & Zhandarov 2003) to a large extent still are phenomenological. Nevertheless these more detailed views support the following assumptions to characterize bond behavior of groups of filaments:

- Outer filaments of a roving mainly follow bond type 2, i.e. bond between filament and matrix, while inner filaments of a roving follow bond type 3, i.e. bond between filaments. So slip effects within a roving have to be considered, and this will be called *slip* in the following.
- Embedding of filaments into the concrete matrix causes a local dissolving of the sizing leading to damage spots and premature failure of single filaments (Sonderforschungsbereich 528 2003). This will be called *filament-defect* in the following.
- Bond characteristics of a filament along its longitudinal axis is not homogenous: some sections with material contact – type 2 or type 3 so called bond bridges – alternate with contact-free sections, both within a span of a part of a mm (Schorn 2003). This will be called *bond-defect* in the following.

Obviously all these effects might lead to a reduced bond efficiency, which leads to a lower load carrying capacity and a reduced ductility of the whole structure.

3 EXPERIMENTAL INVESTIGATIONS WITH TENSION PLATES

3.1 Experimental Setup

A series of displacement-controlled tensile tests were performed by Jesse et al. (2002, 2003). They were carried out on flat specimens of dimension $500 \text{ mm} \times 100 \text{ mm}$ and 8 mm thickness. Fine grained concrete properties have been described in

Section 2.1, as well as glass filament properties. A typical roving consists of 800 filaments, which results in a roving cross section of 0.11 mm^2 . A number of 102 rovings were applied in three layers.

The load is applied by a pivoted wedge clamp in a hydraulic testing machine. The displacement is measured along 200 mm of the edges on both surfaces with a clip-on measuring device. The test speed is 0.015 mm/sec before strain failure. It is controlled by an additional LVDT directly at the ends of the specimen. As a result, displacements in the wedge clamp cannot affect the tests. Figure 3 shows the experimental set-up.

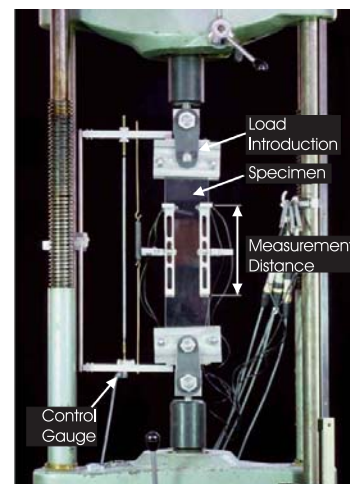


Figure 3. Experimental setup for tension plate.

3.2 Principal results

A typical load-displacement curve is shown in Figure 4, where the load has been related to the plate's cross section leading to a stress and displacement has been related to the measurement length of 200 mm leading to a strain.

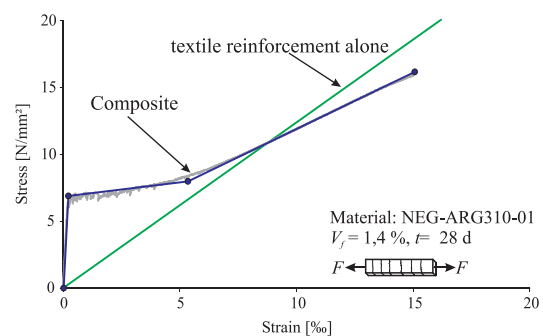


Figure 4. Typical stress-strain curve of experiments.

The stress-strain behavior of textile-reinforced concrete is very similar to that of RC. There are three typical states:

- In the first state the concrete remains uncracked until the tensile strength is reached.
- A state follows in which cracking occurs and the stress-strain curve shows a very flat slope.
- After crack formation is over the stiffness rises again while mobilizing the reinforcement's stiffness.
- A pronounced yielding state does not occur due to the brittle failure characteristics of glass.

Apart from the strong similarities to RC an important property can be observed: after crack formation the stiffness of the composite (line "composite" in Figure 4) is lower compared to the theoretical stiffness, which should be equal to the textile reinforcement standing alone (line "textile reinforcement alone" in Figure 4). This effect – called bundling effect in the following – has to be seen in connection with the complex bond behavior, which as been discussed in Section 2.3, and will be taken up again in Section 4.3.

3.3 Parameter studies

Comprehensive experimental parameter studies have been performed by Jesse et al. (Jesse, Ortlepp & Curbach 2002, Jesse & Curbach 2003), where the influence of ratios of textile reinforcement, fineness of rovings and type of reinforcement (rovings or fabrics of rovings) and types of manufacturing are investigated. The fineness of rovings is measured in tex, which indicates the weight of a roving with a unit length (1 tex = 1 g/km). So a smaller value indicates a finer roving with a higher specific surface area. For sake of comparison a bundle factor is defined as

$$K_B = \frac{m_{II}}{E_f \cdot V_f} \leq 1 \quad (3)$$

where E_f is the Young's modulus of the filament, V_f the reinforcement content and m_{II} gives the slope of the tension plate's stress-strain curve after cracking formation, see Figure 4. Corresponding results are summarized in Figure 5, where K_B is given depending on fineness for different types of reinforcement. As a roving with a lower fineness has a higher specific surface area, the defect mechanisms described in Section 2.3 have a larger influence leading to a smaller effective stiffness or lower bundle factor respectively. Fabrics have a lower

specific surface area, which improves effective stiffness with a higher bundle factor.

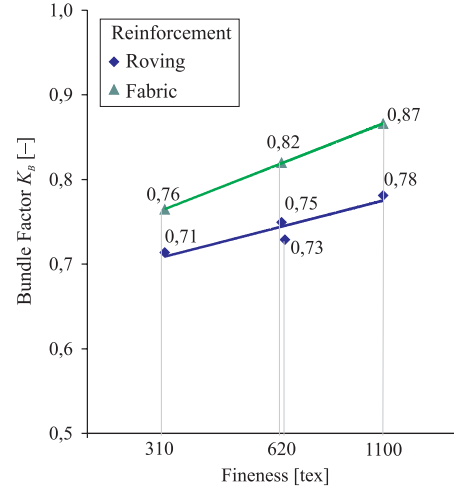


Figure 5. Bundle factor depending on fineness and type of reinforcement.

4 NUMERICAL CALCULATIONS

4.1 Numerical Model

The behavior of the tension plate is modeled by a number of connected bars that is a concrete bar and a number of reinforcement bars. Taking x as the spatial coordinate each bar has its own longitudinal displacement $u_i(x)$ as degree of freedom and a length L . A linear elastic material behavior is assumed for each bar with a limited tensile strength, where different material parameters and different cross section areas are allowed for each bar.

Regarding two arbitrary bars i and j there might be a slip $s_{ij} = u_i - u_j$, which results in bond forces $\tau_{ij} = C_k \cdot f_k(s_{ij})$, where k indicates a particular bond law. Here all bond laws are assumed to follow the general form of Equation (2), but with own parameters τ_m, τ_r, s_1, s_2 .

As a standard case displacement boundary conditions are prescribed for all bars with a zero displacement on the left side and some non zero displacement on the right side, which is increasing from zero to a prescribed final value. This results in an increasing loading according to the actual stiffness of the system. In case of reaching the tensile strength of a particular bar i during the loading process, e.g. in a place $x_{i,u}$, failure is modeled by separating bar i in $x_{i,u}$. Primarily this concerns the concrete bar and activates to a larger extent its

connections to the reinforcement bars or bond respectively. A multiple failure of one bar along its longitudinal axis may also occur with increasing loads.

The mechanical model is transferred to a numerical model with Finite Elements. This is straightforward in dividing each bar in n bar-elements – each with a linear displacement approach – and $n + 1$ nodes. The element properties are directly taken from the mechanical model. With a total number of n_b bars, one concrete bar and $n_b - 1$ reinforcement bars, the total number of nodes amounts to $n_b \cdot (n + 1)$. A constant element length is assumed, so that n_b nodes of different bars share one position x . Bond is discretized by springs between adjacent nodes of different bars. A nonlinear bond characteristic is assumed according to the bond law Equation (2). A sketch of the FE-model is shown in Figure 6.

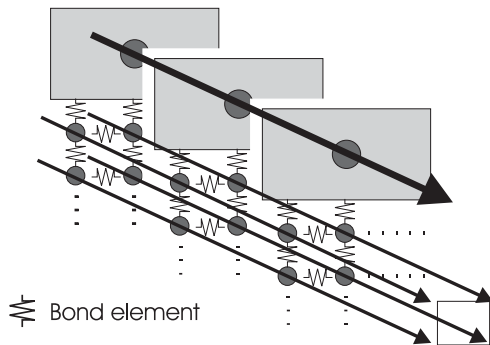


Figure 6. Scheme of FE-model.

According to the mechanical model the FE-model involves nonlinearities with the possibility of a failure of a bar and nonlinear bond elements. Loads or end displacements respectively are applied incrementally, and equilibrium iterations are performed in each load step with the BFGS-method. Using a computer algebra system the program including pre- and post-processing was implemented within a few weeks as a “rapid prototyping” project, going ahead a final C++-implementation. On the other hand the particular CAS leads to some limitations in the problem size.

4.2 Reference case results

First tentative calculations were performed with one concrete bar and up to three reinforcement bars. Geometric dimensions and material parameters follow the experimental tension plate described in

Section 3, where symmetry is used and only one half of the system is discretized. A reference case for the different reinforcement configurations is chosen with a concrete bar and one reinforcement bar, where each bar is modeled with $n = 100$ elements. The parameters are shown in Figure 7.



$$L = 0.1875 / 2 \text{ m}$$

$$A_C = 8.0 \text{ cm}^2 \quad A_R = 0.17 \text{ cm}^2$$

$$C_R = 113 \text{ cm}$$

$$E_C = 30000 \text{ MN / m}^2 \quad E_R = 80000 \text{ MN / m}^2$$

$$f_{Ct} = 7 \text{ MN / m}^2 \quad f_{Rt} = 1500 \text{ MN / m}^2$$

Figure 7. System and parameters of reference case.

The reinforcement ratio of 2 % is slightly different compared to the case of Figure 2, but this has no influence upon the characteristic behavior. As the right part of the tension plate is fixed by the clamps of the experimental machinery, it is assumed, that the right part with a length of 3.75 cm is excluded from tension failure, which results in a free length of 15 cm. This value corresponds to the free length of the experimental plate.

A final target displacement of 0.1875 mm – this corresponds to a mean strain of 1.25 ‰ related to the free length and 1.875 ‰ to the measurement length of the experiments – is applied with 250 increments. As the system is controlled by prescribed displacements the transferred load is a computational result. It proves to be favorable, that in one increment not more than one element is allowed to fail due to exceeding the material tension strength. This together with the finite loading increments leads to pseudo stochastic failure values, i.e. actual failure values of the concrete bar cover a range of 7 - 8 MN/m in the computations.

As with steel reinforcement the textile concrete reference case shows a load-displacement curve with three typical stages:

- Linear elastic behavior of concrete and reinforcement before the tension strength of the concrete is reached.
- Ongoing cracking with a roughly constant load and increasing displacements.

- Final cracking state of concrete with linearly increasing load and displacement, but a reduced stiffness compared to the uncracked state.

The computed load-displacement curve of the reference case is shown in Figure 8, which has to be compared to Figure 4 of the corresponding experimental results.

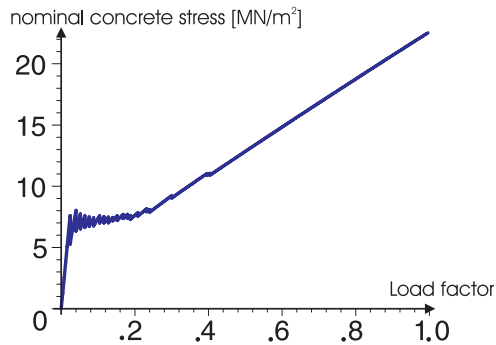


Figure 8. Load-displacement curve for reference case.

The final displacement value corresponds to a maximum reinforcement strain 1.33 % which is reached in a number of 20 cracks within the free length, which leads to a mean crack spacing of 0.75 cm. This is much lower compared to steel reinforcement and results from the very high specific surface of the textile reinforcement.

Well-known characteristic results are also computed for concrete and reinforcement strains. A typical example for the stage of ongoing cracking is shown in Figure 9 with the characteristic reinforcement peak values and vanishing concrete strains in the cracks.

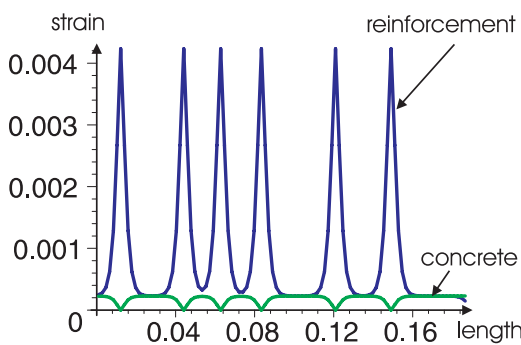


Figure 9. Strains of reference case in a stage of ongoing cracking (load factor 0.12).

Strain differences of concrete and reinforcement correspond to bond stresses. The corresponding

computed values are shown in Figure 10. It can be seen that maximum bond stresses of 10 MN/m² are activated as peak values in this early loading stage.

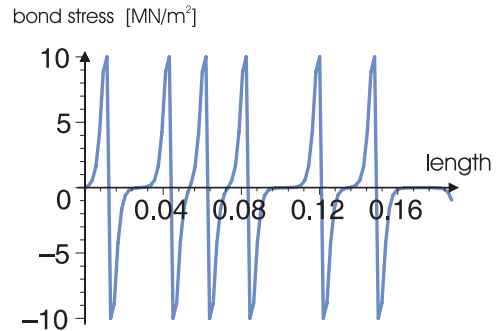


Figure 10. Bond stresses of reference case in a stage of ongoing cracking (load factor 0.12).

4.3 Computational results for bond defects

The reference case shows an ideal behavior, as activation of a reinforcement bar as a whole is enforced by the particular model. A more realistic behavior may differ significantly caused by the defects, which have been discussed before. These effects should be regarded for the mechanical model.

The mechanical model allows for an arbitrary number of reinforcement bars with different bonds laws, see Figure 2. This can be used to regard the different bond defects. In a first approach:

- *Slip*: Two reinforcement bars, where the first bar is connected to the concrete with a filament-concrete bond with parameters $\tau_m=10 \text{ MN/m}^2$, $s_1=5 \mu\text{m}$, $\tau_r=3 \text{ MN/m}^2$, $s_2=100 \cdot s_1$. The second reinforcement bar is connected to the first with a filament-filament bond with parameters $\tau_m=\tau_r=1 \text{ MN/m}^2$, $s_1=s_2=5 \mu\text{m}$.
- *Filament-defect*: Three reinforcement bars, which are all directly connected the concrete bar with a filament-concrete bond. One of the reinforcement bars is assumed to have a reduced tensile strength of 300 MN/m².
- *Bond-defect*: one reinforcement bar, which is directly connected to the reinforcement bar with a filament-concrete bond, not at every node as in all other cases, but at every fourth node.

These are rough approaches, but should give a first qualitative insight of the complex bond behavior of textile concrete.

The extension of the FE-model of the reference case should again be straightforward by adding more reinforcement bars and modifying the bond laws. The total cross section and the total circumference of the reinforcement are unchanged in all cases compared the reference case. The computations are performed in the same way as with the reference case.

4.3.1 Slip results

The computed load-displacement curve is shown in Figure 11: There are some differences in the stage of ongoing cracking with less cracks and a more pronounced saw-tooth effect. The stiffness in the final cracking state is not constant, but slowly decreasing. The final load is reduced by 19% at the same bar end displacement, but this value is influenced by the peak value τ_m of the filament-filament bond law.

The maximum strains in the first reinforcement bar – which is directly connected to the concrete bar – start with 1.23% in the central cracks and increase to 1.82% in the cracks at the bar end. The strains in the second reinforcement bar – which is connected to the first reinforcement bar and not connected to the concrete bar – are considerably lower with a maximum of 0.92% in the central cracks.

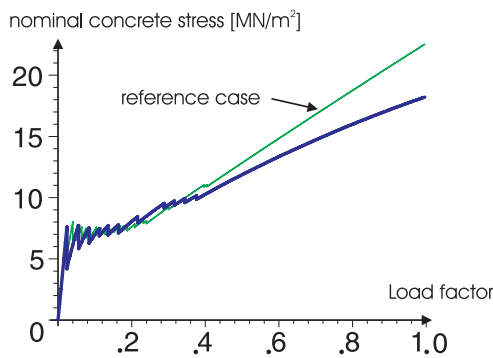


Figure 11. Load-displacement curve for slip.

4.3.2 Filament-defect results

The computed load-displacement curve is shown in Figure 12. There are slight differences in the stage of ongoing crack propagation. The stiffness in the final cracking state is constant but lower compared to the reference case. The final load is reduced by 29% at the same bar end displacement. But this is strongly influenced by the portion of the bars with a reduced strength, while the reduced strength

value has a minor influence. The maximum reinforcement strains reach 1.41%.

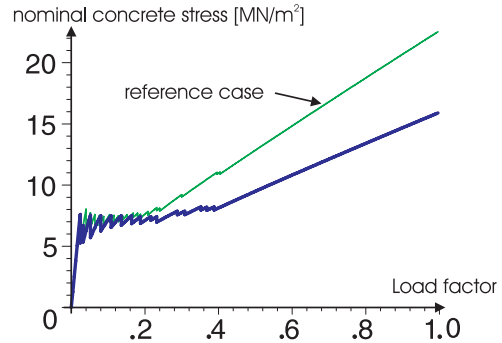


Figure 12. Load-displacement curve for filament-defect.

4.3.3 Bond-defect results

The computed load displacement curve is shown in Figure 13. Crack spacing is considerably higher compared to the other cases. The stiffness in the final cracking state is nearly constant but lower compared to the reference case. The final load is reduced by 12% at the same bar end displacement. This value may be moderately influenced by portion of reinforcement elements, which are directly connected to the concrete. The maximum reinforcement strains are 1.18%.

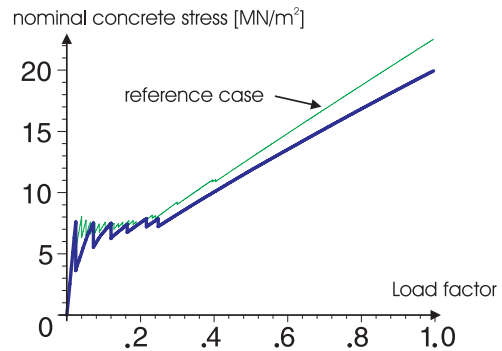


Figure 13. Load-displacement curve for bond-defect.

4.3.4 Assessment

The quantitative results of the different cases, e.g. the stiffness decrease after multiple cracking, may be influenced by the key parameter of each case, i.e. the peak value τ_m of the filament-filament bond law in case of slip, the portion of bars with a reduced strength in case of filament defect, and the portion of bonded elements in the case of bond-defect. On the other hand some qualitative results, e.g. distance of cracks or stiffness characteristics after multiple cracking, give an indication, that the fila-

ment-defect gives a major contribution to the overall behavior of the tension plate. But this result has to be further validated.

5 CONCLUSIONS

Current investigations show, that multifilament yarns used as reinforcement in concrete do not reach their theoretical capabilities with respect to stiffness and load carrying capacity. It is generally accepted, that the reasons have to be seen in connection with the quite complex bond behavior. So a number of hypotheses have been proposed about the bond behavior of rovings in fine grained concrete. As the current state of experimental research does not give sufficient material to verify these different hypotheses, additional theoretical investigations with numerical calculations have to be considered. First tentative results support the assumption that the reduction in stiffness is primarily caused by the failure of the outer filaments of a roving. This may be forced additionally by the decreased strength of these filaments, as they are particularly exposed to alkali attack of the surrounding concrete. This has to be proved in further investigations with more refined mechanical models and large scale numerical parameter studies.

REFERENCES

- Banholzer, B. 2001. Zum Mechanismus des Pull-Out-Versuches von Garnen aus einer zementgebundenen Matrix. In: Hegger, J. (ed.), *Textilbeton – 1. Fachkolloquium der Sonderforschungsbereiche 528 und 532, 15.-16.2.2001*. Institut fuer Massivbau, RWTH Aachen, Germany: 99-112.
- Bartos, P. 1980. Analysis of pull-out tests on fibres embedded in brittle matrices. *Journal of Materials Science* 15: 3122-3128.
- Bramshuber, W. & Banholzer, B. 2003. Bond characteristics of filaments embedded in fine grained concrete. In: Curbach, M. (ed.), *Textile Reinforced Structures. Proceedings of the 2nd Colloquium on Textile Reinforced Structures (CTRS2), Dresden, Germany, 29.9.2003–1.10.2003*: 63-76.
- Butler, W. & Schorn, H. & Hempel, R. & Schiek, M. 2003. Untersuchungen zur Dauerhaftigkeit von alkaliresistenten Glasfilamentgarnen in zementgebundenen Matrices. In: Curbach, M. (ed.), *Textile Reinforced Structures. Proceedings of the 2nd Colloquium on Textile Reinforced Structures (CTRS2), Dresden, Germany, 29.9.2003–1.10.2003*: 77-89.
- Curbach, M. & Brückner, A. 2003. Textile Strukturen zur Querkraftverstärkung von Stahlbetonbauteilen. In: Curbach, M. (ed.), *Textile Reinforced Structures. Proceedings of the 2nd Colloquium on Textile Reinforced Structures (CTRS2), Dresden, Germany, 29.9.2003–1.10.2003*: 347-360.
- Jesse, F. & Ortlepp, R. & Curbach, M. 2002. Tensile Stress-Strain Behaviour of Textile Reinforced Concrete. In: *Proceedings of the IABSE Symposium, "Towards a better built environment - innovation, sustainability, information technology"*, Melbourne. IABSE, ETH-Zurich, Switzerland.
- Jesse, F. & Curbach, M. (2003). Strength of Continuous AR-Glass Fibre Reinforcement for Cementitious Composites. In: Naaman, A. E. & Reinhardt, H.-W. (eds.): *High Performance Fibre Reinforced Cementitious Composites HPRFCC-4. Proceedings of the Fourth International RILEM Workshop*. Bagnaux, France, RILEM Publications: 337-348.
- Littwin, R. 2001. Verifizierung und Optimierung eines Verbundgesetzes. In: Hegger, J. (ed.), *Textilbeton - 1. Fachkolloquium der Sonderforschungsbereiche 528 und 532, 15.-16.2.2001*. Institut fuer Massivbau, RWTH Aachen, Germany: 137-150.
- Ortlepp, R. & Curbach, M. (2003). Bonding behavior of textile reinforced concrete strengthening. In: Naaman, A. E. & Reinhardt, H.-W. (eds.): *High Performance Fibre Reinforced Cementitious Composites HPRFCC-4. Proceedings of the Fourth International RILEM Workshop*. Bagnaux, France, RILEM Publications: 517-527.
- Schorn, H. 2003. Ein Verbundmodell für Glasfaserbewehrungen im Beton. In: *Bautechnik*, No. 3, p. 174-180
- Sonderforschungsbereich 528 (Edt.), 2003. *Zwischenbericht zur Dauerhaftigkeit und Dauerstandfestigkeit von textiler AR-Glasfaserbewehrung im Beton*. – in preparation
- Reinhardt, H.-W. & Krüger, M. 2001. Vorgespannte dünne Platten aus Textilbeton. In: Hegger, J. (Edt.), *Textilbeton – 1. Fachkolloquium der Sonderforschungsbereich 528 und 532*. Aachen : Lehrstuhl und Institut für Massivbau, Mies-van-der-Rohe-Str. 1, 52074 Aachen. p. 165-174
- Zhandarov S. & Mäder, E. 2003. Characterization of Fibre/Matrix Interface Properties: Applicability of Different Tests, Approaches and Parameters. In: Curbach, M. (Edt.): *Textile Reinforced Structures. Proceedings of the 2nd Colloquium on Textile Reinforced Structures (CTRS2), Dresden, Germany, 29.9.2003–1.10.2003*, Dresden : Sonderforschungsbereich 528, Technische Universität Dresden, 2003: 101-120.